

Extraction of a Check-Reversal Visual Evoked Potential under Conditions of Simulated Nystagmus

Avery H. Weiss^{1,2}, John P. Kelly^{1,2} and James O. Phillips^{1,3}

¹Seattle Children's Hospital, Division of Ophthalmology, Seattle, Washington, USA

²University of Washington Medical Center, Department of Ophthalmology, Seattle, Washington, USA

³University of Washington Medical Center, Department of Otolaryngology, Seattle, Washington, USA

23.1 Introduction

Infantile nystagmus is the onset of involuntary ocular oscillations within the first 6 months of life (Leigh & Zee 1991; Abadi & Bjerre 2002; Dell'Osso & Daroff 2007). It can be an isolated ocular motor abnormality in which the visual sensory system is normal. Infantile nystagmus can be associated with a defect in the visual system including opacities of the ocular media (cornea, lens, or vitreous) and functional abnormalities of the macula (albinism and aniridia), retina (Leber's congenital amaurosis) or optic nerve. Visual sensory disorders must be bilateral and present before 6 months of age to be associated with infantile nystagmus. Ocular oscillations due to infantile nystagmus are usually conjugate and horizontally directed in primary and eccentric gazes but vertical or torsional components can be present.

During visual development, the amplitude and velocity profile of the nystagmus can undergo substantial changes (Reinecke *et al.* 1988; Gottlob 1997; Hertle *et al.*

The Challenge of Nystagmus. Edited by Chris Harris, Irene Gottlob and John Sanders. © 2012 Nystagmus Network. Published 2012 by Nystagmus Network.

2002). Post-natal modifications of the waveform include variable reductions in amplitude and frequency of the nystagmus, and transformation of a pendular waveform to an asymmetric pendular or jerk waveform. Emergence of a high velocity component aligns the object of interest on or near the fovea for a short interval known as the “foveation period.” During the foveation period eye velocity is at a minimum and extraction of high spatial frequency information from a stimulus in motion is maximized. This notion is supported by the finding that visual acuity is correlated with the slow-velocity components of the nystagmus (Abadi & Worfolk 1989; Bedell 2000; Dell’Osso *et al.* 2007) and acuity decreases as retinal image motion increases. (Westheimer & McKee 1975; Kelly 1979; Demer & Amjadi 1993).

Objective visual electrophysiology is important to identify a visual sensory defect associated with infantile nystagmus during early childhood (Brodie 1991; Shawkat *et al.* 2000, 2001, Breclj & Stirn-Kranjc 2004). The most practical approach to objective visual system assessment is the visual evoked potential (VEP). However, check-reversal stimulation, a standard method of generating the VEP, elicits a severely degraded or absent response in observers with infantile nystagmus (Creel *et al.* 1981; Apkarian and Shallo-Hoffmann 1991; Saunders *et al.* 1998). Previous work has shown that the severe reduction in the check-reversal VEP can be explained by the retinal slip, or stimulus motion, induced by the nystagmus (Arlt & Zangemeister 1990; Hoffmann *et al.* 2004). In these experiments, a normal observer views a checkerboard reversing pattern while the stimulus is horizontally oscillated at constant velocity in a saw-tooth movement. VEP amplitude was not reduced if the stimulus was presented in an appearance-disappearance mode. Hoffman *et al.* (2004) suggested selective reduction to the check-reversal response under simulated saw-tooth nystagmus was due to motion adaptation, which reduces VEP amplitude (Bach & Ullrich 1994; Hoffmann *et al.* 1999; Heinrich & Bach 2001). The cancellation of the VEP response could not be explained by the temporal and spatial coincidence of the simulated movement and the check reversal.

In this study, we recorded VEP responses to a check-reversal stimulus that was moving at the same velocity as the eye movements of a subject having isolated infantile nystagmus. That is, subjects with normal visual sensory function and stable gaze holding viewed stimuli moved in a manner experienced by actual infantile nystagmus observers. To explore further the underlying basis for the reduced check-reversal VEP, we examined the relationship between the VEP and velocity-specific components of the eye movement using a novel cross correlation analysis. This analysis attempts to isolate cortical responses generated in response to discrete epochs of retinal image motion that could be overlooked by averaging at the check-reversal rate.

23.2 Methods

23.2.1 Subjects

Subjects were five adult observers (two males, three females, age range 29–53 years) with normal vision and stable fixation. All had acuity that could be corrected to 20/20 or better.

The research followed the tenets of the World Medical Association Declaration of Helsinki, and informed consent was obtained from the subjects after explanation of the nature and possible consequences of the study.

23.2.2 Stimulus

Stimuli were presented on an Eizo TX-C7 raster monitor subtending $22.8^\circ \times 17.3^\circ$ (width \times height) at 77 cm viewing distance under monocular viewing (the eye chosen at random). Each pixel was 0.036° and the frame rate was 60 Hz (set to match the eye movement recording rate, see below). Mean luminance was kept at 52 cd/m^2 and Michelson contrast was 80% throughout the experiment. Checkerboard-reversal stimuli were either 42 or 84 arcminutes, both undergoing square-wave contrast modulated at 2.74 reversals per second. (Three of the five subjects were also tested with the 42 arcminute stimulus.) To maintain central and stable fixation, a small target of ($\sim 0.1^\circ$ subtense) was placed in the middle of the screen. The visual stimulus was generated by custom PC software written by one of the authors (JPK).

Each subject had their eye movements simultaneously recorded using the electro-oculogram to ensure gaze holding was stable. Sessions with unstable fixation were rejected and recorded again. Electroencephalography (EEG) epochs without stable fixation were rejected before data analysis. Nystagmus waveforms used to move the stimuli were created from 60 Hz video-oculography recordings (Sensorimotoric Instruments, Berlin, Germany) from the left eye of a pediatric patient with infantile nystagmus without an associated visual sensory defect. The patient was a 12-year-old female with 20/25 acuity and normal ocular fundus, but exhibited a 5 Hz conjugate horizontal asymmetric pendular nystagmus of about 5° amplitude. Slow-phase velocities ranged from near 0 to more than $60^\circ/\text{s}$; 18% of the recording contained epochs (16–70 ms) of slow velocity less than $2^\circ/\text{s}$. The data from video-oculography recording was converted into pixel equivalent shifts in horizontal space for the display and refreshed at 60 Hz to match the temporal properties of the display screen with the eye movement recording. The recording used in the simulated nystagmus was 15.75 s and was doubled in duration to ensure adequate time for averaging of the VEP response.

23.2.3 VEP recording and analysis

Scalp VEPs were recorded by a NeuroScan system (Compumedics USA, Charlotte, North Carolina, USA) using Grass gold-cup surface electrodes. Skin preparation and electrode application followed standard procedures. A reference electrode was placed at the vertex (Cz in the 10–20 classification) and active electrodes were placed at Oz (3.5–4 cm above the Inion). An electrode between Oz and Cz served as ground. (Of note, our recordings are based on our own normative database protocols, which depart from strict International Society for Clinical Electrophysiology of Vision (ISCEV) standards that specify Fz as a reference and Cz as a ground.) Impedance was between 8 and 17 k Ω . The EEG was filtered from 0.05 to 100 Hz, and digitized at 500 Hz. The EEG and electro-oculography were amplified 5000 times and bandpass filtered (0.05–100 Hz bandpass). The VEP response was an averaged to 80 check reversals under no simulated nystagmus (static) viewing conditions and the VEP response was an average of 110–168 check reversals under simulated nystagmus (dependent on stable fixation). Amplitude of the VEP was defined by the voltage difference between the predominant positive peak (P100 for the peak near 100 ms) to the preceding negative peak. Latency was defined as the time from the stimulus onset to the peak of predominant positive peak.

To extract a response that was associated with specific components of the stimulus motion, a cross-correlation of the EEG was performed with a sequence of timed events:

$$r(\tau) = \frac{1}{s} \sum_{i=1}^{N-1} \text{EEG}(i) y(i + \tau), \tau = 0, 1, 2, \dots, \delta.$$

where each discrete sample point i in the EEG record of length N is multiplied by the sequence function $y(\cdot)$ with delay of τ and duration $\delta = 150$ sampled points. The sequence function is an array of 1s and 0s that are temporally aligned on a point of interest. The value s is the sum of the sequence function. For example, to extract the response to the check reversal, the sequence function $y(\cdot)$ would have a 1 at each point in time that a reversal occurred and 0 at all other times, therefore, $r(\tau)$ would be the same as the averaged check-reversal response. After the cross correlation analysis, all VEP responses were digitally bandpass filtered from 0.5 to 35 Hz.

Figure 23.1 shows the simulated nystagmus waveform aligned with the sequence function that extracts the VEP response at specific points. The top trace is the stimulus position that simulates the nystagmus eye movement. The second trace is a function that has a value of 1 immediately after a leftward fast phase followed by a brief period of relatively stable slow phase (presumed “foveation period”).

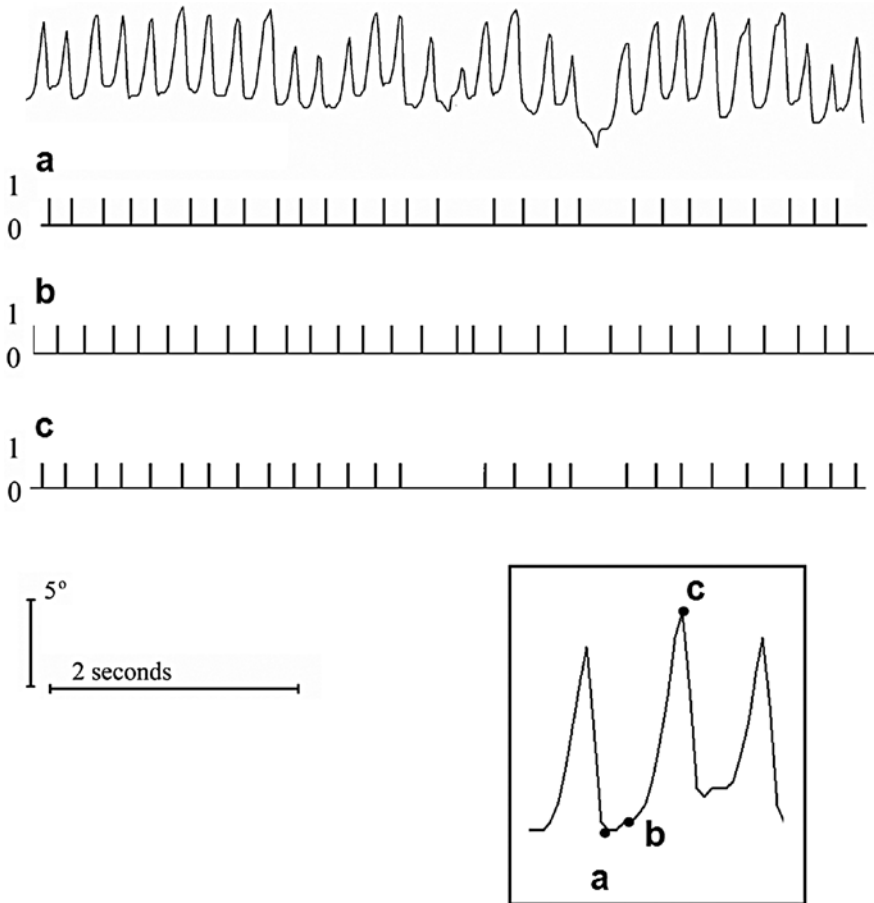


Figure 23.1 A segment of the horizontal eye position trace used to simulate image retinal slip due to nystagmus. Upward and downward deflections represent right and left directions, respectively. Below the position trace are three sequence functions of 1s and 0s convolved with the EEG to derive VEP components at specific points of the simulated nystagmus. The sequence extracts the response at the start of the slow phase (a), the transition in the slow phase (b), and the end of the slow phase (c).

This analysis will extract the VEP response at the start of the slow-phase component. Each point meeting these criteria was identified by the presence of a preceding eye velocity greater than $32^\circ/\text{s}$ (fast phase) followed by 50 ms of velocity less than $11^\circ/\text{s}$ (slow phase). There were 88 points meeting criteria, all remaining points were assigned a value of zero. A second sequence function applied to the same simulated nystagmus is shown in the third trace. This sequence function extracts the VEP response to the transition of the slow phase. Each point meeting criteria was characterized by a stimulus velocity $0\text{--}31^\circ/\text{s}$ to the left followed by 33 ms of stimulus velocity greater than $32^\circ/\text{s}$ to the right. There were 107 points meeting criteria. A third sequence function, applied to the same simulated nystagmus, is shown in the fourth trace. This sequence function extracts the VEP response at the end of the slow phase. Each point meeting criteria had a preceding eye velocity less than $11^\circ/\text{s}$ followed by 67 ms of rightward velocity of 33 to $90^\circ/\text{s}$. There were 127 points meeting criteria. Figure 23.1 (inset) depicts the corresponding extraction points on a segment of the simulated nystagmus. Note that the sequence functions are not consistently rhythmic, in which case the analysis is less likely to extract an unrelated signal due to synchronous background EEG, such as alpha or beta rhythm. To ensure the extracted responses were unrelated to synchronous background EEG, the same extraction analysis was performed on each subject's EEG during the intervals between stimulus presentations: that is, when the subject was viewing a blank stimulus monitor of the same mean luminance.

23.3 Results

The VEP responses from the five subjects to standard check reversal of 84 arc-minute checks are shown at the top left of Figure 23.2a. All subjects show typical appearing VEP responses with the predominant positive peak appearing near 100 ms (P100). The P100 amplitude ranged from 6.7 to 15.5 μV . The P100 latency varied from 98 to 106 ms. Under the condition where check reversal was moved by simulated nystagmus (Figure 23.2b), all subjects had a reduced P100 peak that was indistinguishable from background noise and therefore could not be scored for amplitude and latency.

Figure 23.2c shows the VEP responses extracted during the start of the slow phase of the simulated nystagmus (each response is an average to 88 epochs). Figure 23.2d shows the VEP responses extracted at the end of the slow phase (each response is an average to 127 epochs). Both responses were characterized by a broad peak of long latency. For the start of the slow phase, peak amplitude was 5.3–8.1 μV and was significantly lower than that recorded to standard check reversal ($p = 0.03$). Latency varied between 160 to 190 ms and was significantly longer than that recorded to standard check reversal ($p = 0.0002$). For the end of the slow phase, peak amplitudes ranged from 4.6 to 7.1 μV and latency ranged from 194

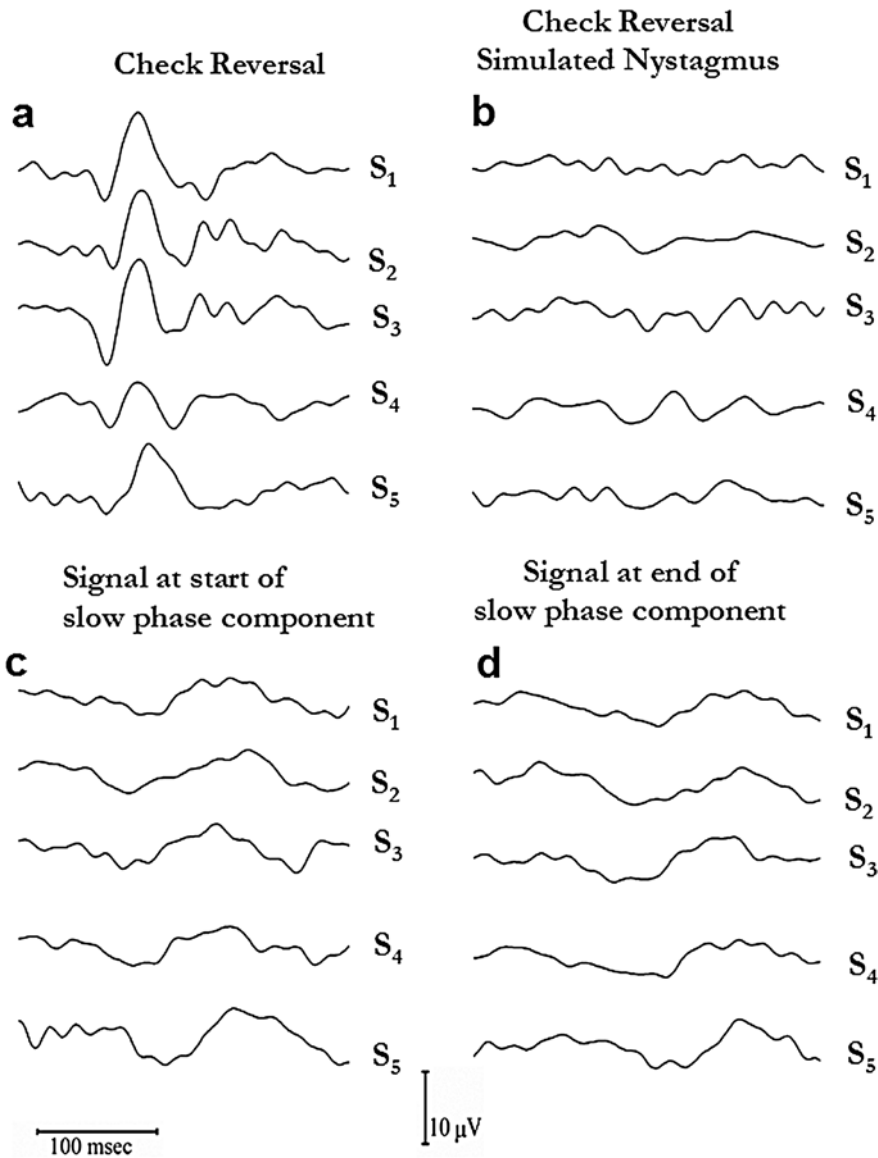


Figure 23.2 VEP responses from five subjects while viewing contrast reversing checkerboards of 84 arc minutes. (a) Standard check reversal under stationary viewing. (b) VEP response when the check-reversal stimulus is horizontally moved identical to eye movements recorded from a subject with infantile nystagmus. (c) Extracted response using the sequence function in Figure 23.1a, which averages at the start of the slow phase of the simulated nystagmus. (d) Extracted response using the sequence function shown in Figure 23.1b, which averages at the end of the slow phase of the simulated nystagmus. Except for the standard check-reversal response at the top left, all VEPs were obtained from the same recording.

**Extracted VEP to blank stimulus using two
sequence functions.**

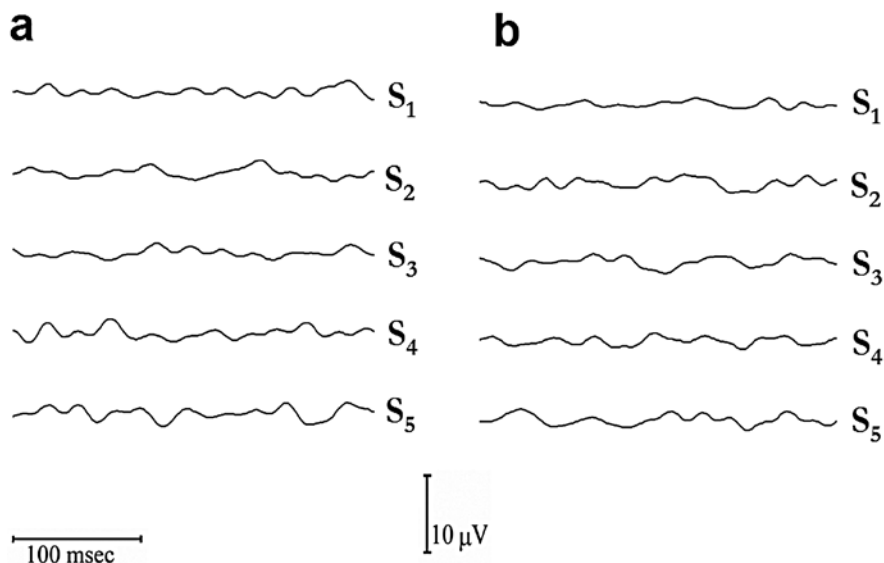


Figure 23.3 Extracted VEP responses from five subjects while viewing a blank screen of the same mean luminance as the contrast reversing checkerboards. (a) Extracted response using the sequence function in Figure 23.1a (start of the slow-phase component). (b) Extracted background noise using the sequence function shown in Figure 23.1b (end of the slow-phase component).

to 218 ms. Amplitude was significantly lower ($p = 0.02$) and latency significantly longer ($p = 0.00003$) than standard check reversal.

Figure 23.3 shows extracted VEP responses, using the same sequence functions as in Figure 23.1a, b while subjects were viewing monitor of the same mean luminance but without a check-reversing pattern. The EEG was appended between stimulus presentations and then underwent the same cross correlation analysis. This extracted unrelated synchronous background EEG related to the timing of the sequence function and thus served as an index of background noise. Extracted responses were much smaller than extracted responses to the check-reversing pattern undergoing simulated nystagmus.

To account for inter-subject variations in amplitude, each subject's VEP to the standard check reversal was scaled to 1.0 at the P100 peak. The same scale factor for each subject was then used to normalize the amplitude in each of the remaining test conditions. The normalization provides the relative change in amplitude that

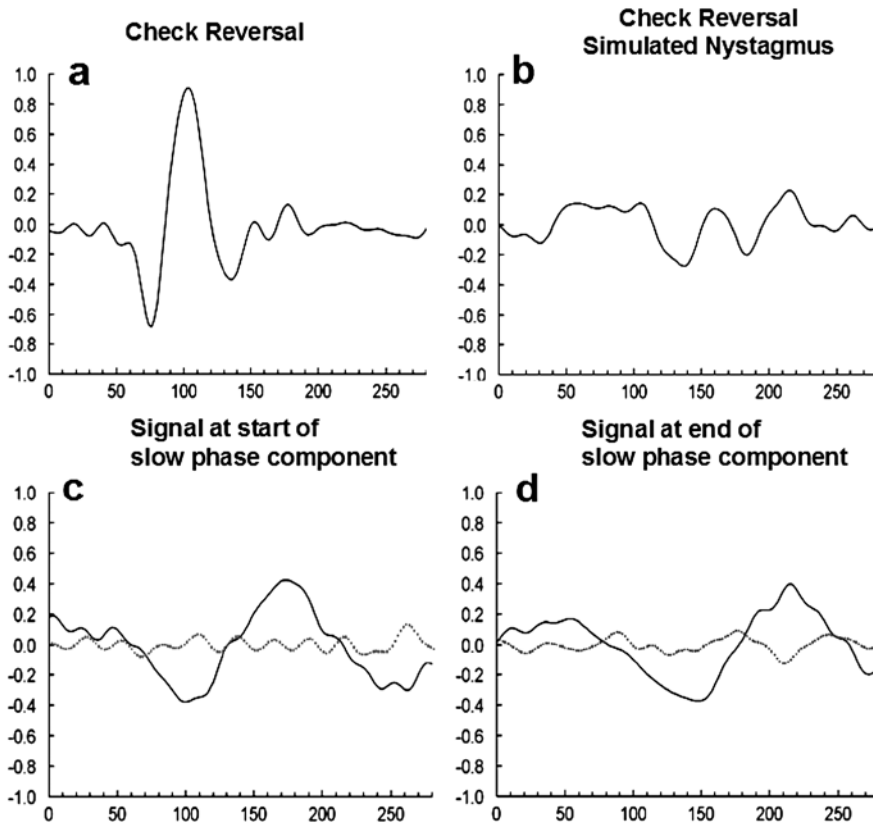


Figure 23.4 For each subject, VEPs were normalized to 1.0 at the peak to standard check reversal, then this normalization factor was applied to each subject's extracted VEP waveform. Check size is 84 arcminutes. (a) Standard check-reversal (stationary display). (b) Check-reversal VEP under simulated nystagmus. (c, d) Extracted responses at the start and end of the slow phase of the simulated nystagmus, respectively. The thin gray lines in (c) and (d) show the extracted background noise from the sequence functions. The abscissa is time in milliseconds.

could be averaged across subjects without biasing the results by individual subjects with large amplitude. Figure 23.4 shows the averaged VEP response across all subjects after normalization. Under the simulated nystagmus condition, the averaged VEP shows a small peak near 150 ms that is approximately 20% of the standard check-reversal response.

Figure 23.4c shows the VEP responses extracted during the start of the slow phase of the simulated nystagmus (each response is an average to 88 epochs).

Figure 23.4d shows the VEP responses extracted at the end of the slow phase (each response is an average to 127 epochs). Both the extracted responses from the start and end of the slow-phase component show a broad peak of approximately 50% of the standard check-reversal response. Latency was 175 and 215 ms for the start and end of the slow-phase component, respectively. The thin lines in Figure 23.4c, d shows the normalized VEP responses while the subject viewed the monitor of the same mean luminance but without a check-reversing pattern.

Figure 23.5 shows that normalized VEPs averaged across subjects were similar between 84 and 42 arcminute checks. There was a reduced response to simulated

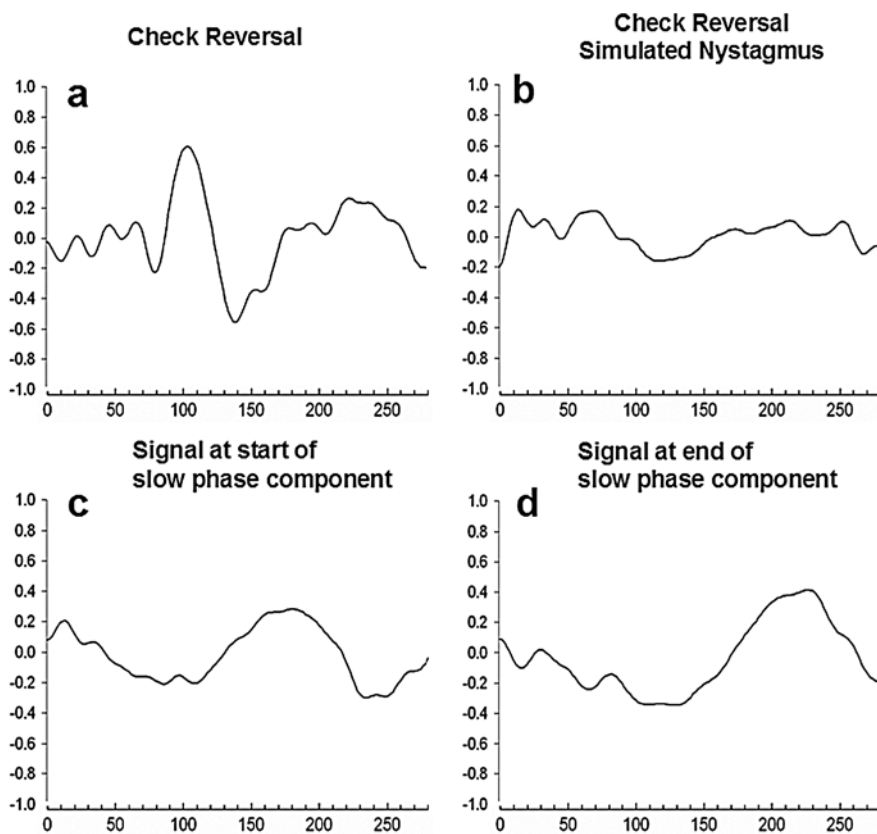


Figure 23.5 Same conventions as Figure 23.3, except check size is 42 arcminutes (dark lines). The responses from the 84 arcminute check condition are superimposed on the data (thin gray lines)

nystagmus (Figure 23.5b) but a relatively larger peak of long latency that was extracted from the start and end of the slow-phase (Figure 23.5c, d, respectively). The amplitude under the simulated nystagmus condition showed a small residual peak of approximately 10% of the standard check-reversal response near 170 ms. Compared with the standard check-reversal response, the extracted response at the start of the slow phase was 50% of the standard check-reversal VEP. For the extracted response at the end of the slow phase, the amplitude was about 40% lower than the standard check-reversal VEP. Latency to the predominant peak was 180 and 225 ms for the early and late components, respectively.

We then examined the relationship between specific epochs of the slow velocity component and the extracted VEP responses. The top of Figure 23.6 depicts three different points on the nystagmus waveform that were used to extract the response. Point **b** represents the start of the slow-phase, point **a** corresponds to the transition between the low and high velocities of the slow phase. Finally point **c** corresponds to the end of the slow phase. The figure shows the averaged normalized amplitudes for each of these points in time (number of epochs for averaging are **a** = 107, **b** = 88, and **c** = 127). Extracted VEPs to larger check stimuli are shown on the left column and to smaller checks are shown on the right column. Note that the response extracted at point **a** has a short latency near 88 ms but that points **b** and **c** have peaks that are later in time. The average time delays for points **a**, **b**, and **c** cover one cycle of nystagmus and are shown by the arrows on the abscissa. The observed peak of the extracted VEP response is close, but not exactly aligned to the average timing for each corresponding point in the nystagmus waveform. This analysis suggests that a VEP response can be extracted from each point of the slow phase in the motion stimulus. However, the latency of each point seems to vary according to its temporal relationship to the fast phase and the slow eye velocities that follow. As evidence, the transition point follows a saccade and a sustained epoch of slow eye velocity and has the shortest latency. After correcting for the average duration of the saccade (66 ms), the latency of point **b** is within 10 ms of point **a**. In comparison, point **c** has a latency of 150 ms after correcting for the average duration of the saccade.

To test for a motion specific response in the extracted VEP responses, a control experiment was performed in which the subject viewed the 84 arcminute check stimulus under simulated nystagmus but without any contrast reversal. The results of this control experiment are shown in Figure 23.7. Dark lines are for stimuli with reversing checks and gray lines are for check stimuli that do not undergo contrast reversal. At top (A) are test-retest results of the check-reversal response for comparison. The following graphs show extraction of the VEP signal at the start of the slow phase (B), VEP at the end of the slow phase (C), and at the transition of slow phase (D). The bottom graph estimates the noise level, which is the VEP average on what would be the standard check-reversal rate. The VEP responses are very

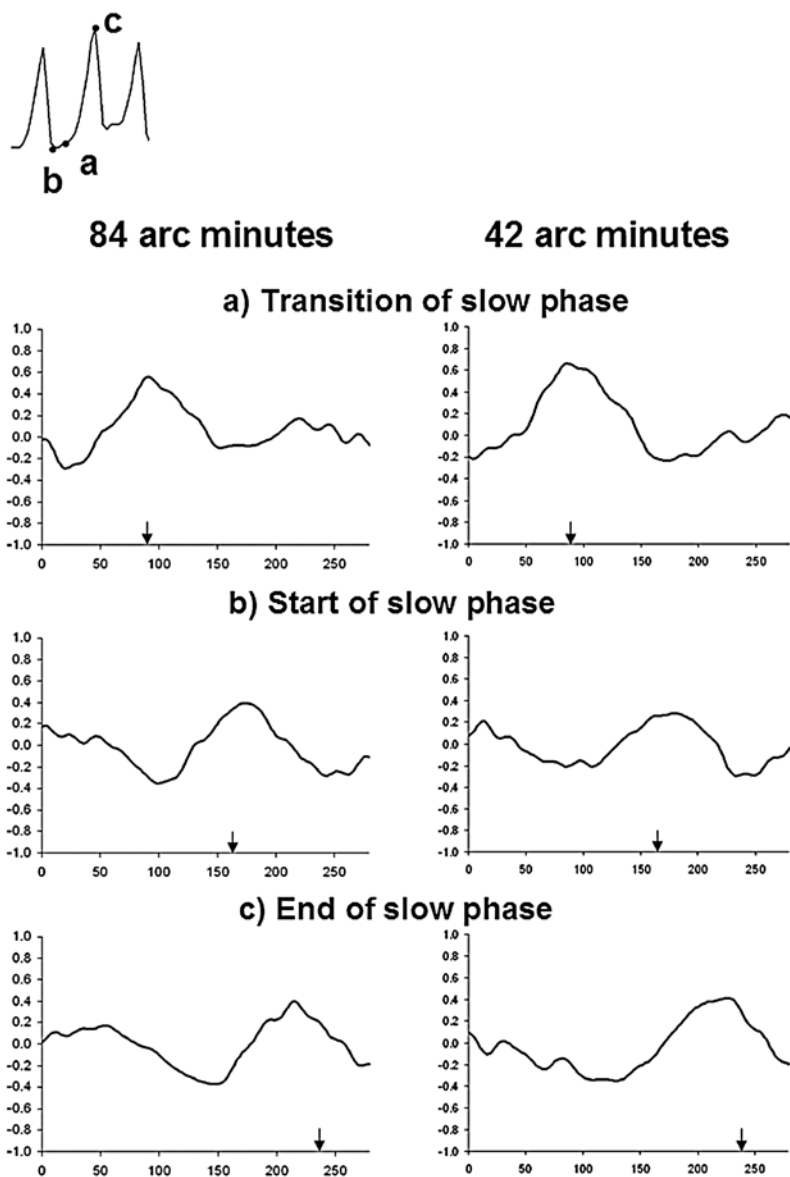


Figure 23.6 Normalized VEP responses aligned to points in the simulated nystagmus at (a) the transition from the start to end of the slow phase, (b) the start the slow phase, and (c) end of the slow phase. Left and right columns are for 84 and 42 arcminutes, respectively. The arrows show the average time delay between points **a** to **b**, and **a** to **c** in the simulated nystagmus. The abscissa is time in milliseconds.

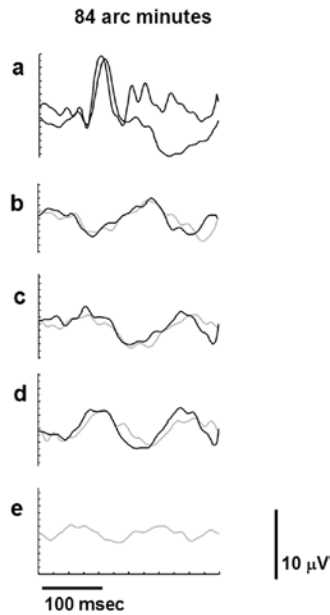


Figure 23.7 Dark lines are for stimuli with reversing checks and gray lines are for check stimuli that do not undergo contrast reversal. Data are from one subject. (a) Test–retest of standard check reversal under stationary viewing. Below are extracted VEP responses aligned to points in the simulated nystagmus at (b) the start the slow phase, (c) end of the slow phase, and (d) the transition from the start to end of the slow phase. (e) shows the VEP response to a noise condition in which the response is averaged on what would be the standard check-reversal rate.

similar between the contrast reversing and non-contrast reversing experiments, indicating that a motion cue generates the extracted response.

23.4 Discussion

We demonstrate that a VEP response to a check-reversal stimulus in motion is selectively generated during the slow-phase of simulated nystagmus in normal subjects. In addition, we confirm that the VEP is severely reduced when the response is averaged across the entire profile of the nystagmus (Arlt & Zangemeister 1990; Saunders *et al.* 1998; Hoffmann *et al.* 2004; Hoffmann & Seufert 2005). Taken together, these data indicate that a salient feature of the check–reversal pattern is preserved and selectively elicits a VEP response when retinal image

motion is relatively stable. The extracted VEP response is likely elicited by the luminance contrast and/or motion of the edges within the checkerboard stimulus.

The generator of the check-reversal VEP is likely the static position of luminance contrast at the edges of the check pattern. Luminance contrast of a black/white checkerboard that is stationary is narrowly distributed across the edges of each check and approaches the 80% contrast in this study. We hypothesize that the luminance contrast of a drifting checkerboard is also broadly distributed across the edges of the rapidly moving black/white checks at the time of the reversal. Given that the strength of the VEP signal is proportional to the luminance contrast at the time of the reversal, the VEP signal will be reduced. The same mechanism may underlie the reduced VEP response observed in infantile nystagmus.

Stimulus motion is another possible source for the observed VEP responses. The motion cue is generated by the spatial displacement of the black/white edges of individual checks that occur during the simulated nystagmus and during the programmed phase reversal. Retinal image velocities simulated in this study ranged from near zero to 60°/s, velocities well within the detection range of the visual motion system. However, the motion signal is convolved with a repetitive spatial pattern also defined by luminance contrast. Therefore the extraction of motion from a moving checkerboard is potentially constrained by spatial frequency. The large size of the checks (1.4°, 07°) and the presence of low velocities (<2°/s) for nearly 20% of the time suggests the distribution of edge contrast is relatively preserved and could generate the VEP. To explore this possibility, we recorded the VEP during simulated nystagmus conditions but without reversing the contrast of the checks. The extracted VEP response was similar under both conditions, suggesting that a component of the extracted VEP is generated by stimulus motion.

The contrast-reversing stimulus has both vertical and horizontal motion components. At each reversal, the parallel edges of a 1° check are also displaced vertically 1°, thereby generating vertical motion. The possibility that the observed extracted VEP response represents a response to vertical motion cannot be completely excluded but it is unlikely. A vertical motion component is present in the contrast reversing stimulus but not in the non-reversing stimulus (horizontal motion only). Therefore, a vertical motion component in the extracted VEP is unlikely because the extracted responses are similar to both reversing and non-reversing stimuli in Figure 23.7.

Latency of the extracted VEP component was related to an antecedent simulated saccade and the low-velocity component of slow-phase component. Differences in VEP latency between fast- and slow-phase components could be accounted for by the average difference in latency between points at the beginning, transition, and end of the slow-phase component. Assuming normal observers have a foveation period in the simulated nystagmus, our finding suggests that the slow-velocity component of our moving stimulus after a presumed foveating saccade is the

source of the extracted VEP. In comparison, latency was prolonged when the VEP was sampled at the end of the accelerating velocities of the slow-phase when the stimulus is presumably the farthest from the fovea. After correcting for the saccade duration (66 ms), latency was still delayed by more than 50 ms. One possible explanation for this latency difference is that the short latency response is generated by the initial slow velocity component while the longer latency response is generated by the later high-velocity component.

References

- Abadi RV, Bjerre A (2002) Motor and sensory characteristics of infantile nystagmus. *British Journal of Ophthalmology* **86**: 1152–1160.
- Abadi RV, Worfolk R (1989) Retinal slip velocities in congenital nystagmus. *Vision Research* **29**: 195–205.
- Apkarian P, Shallo-Hoffmann J (1991) VEP projections in congenital nystagmus; VEP asymmetry in albinism: a comparison study. *Investigative Ophthalmology & Visual Science* **32**: 2653–2661.
- Arlt A, Zangemeister WH (1990) Influence of slow eye movements and nystagmus on pattern induced visual evoked potentials. *Neuro-Ophthalmology* **10**: 10241–10251.
- Bach M, Ullrich D (1994) Motion adaptation governs the shape of motion-evoked cortical potentials (motion VEP) *Vision Research* **34**: 1541–1547.
- Bedell HE (2000) Perception of a clear and stable visual world with congenital nystagmus. *Optometry and Vision Science* **77**: 573–581.
- Brecelj J, Stirn-Kranjc B (2004) Visual electrophysiological screening in diagnosing infants with congenital nystagmus. *Clinical Neurophysiology* **115**: 461–470.
- Brodie SE (1991) Choice of initial tests for nystagmus in infants. *Archives of Ophthalmology* **109**: 464.
- Creel D, Spekrijse H, Reits DT (1981) Evoked potentials in albinos: efficacy of pattern stimuli in detecting misrouted optic fibers. *Electroencephalography and Clinical Neurophysiology* **52**: 595–603.
- Dell'Osso LF, Daroff RB (2007) Nystagmus and saccadic intrusions and oscillations. In: Tasman W & Jaeger EA (eds) *Duane's Ophthalmology*, electronic edition. Philadelphia, PA: Lippincott Williams & Wilkins.
- Demer JL Amjadi F (1993) Dynamic visual acuity of normal subjects during vertical optotype and head motion. *Investigative Ophthalmology & Visual Science* **34**: 1894–1906.
- Gottlob, I. (1997) Infantile nystagmus. Development documented by eye movement recordings. *Investigative Ophthalmology & Visual Science* **38**: 767–773.
- Heinrich, SP, Bach, M (2001) Adaptation dynamics in pattern-reversal visual evoked potentials. *Documenta Ophthalmologica* **102**: 141–156.
- Hertle RW, Maldonado VK, Maybodi M, Yang D (2002) Clinical and ocular motor analysis of the infantile nystagmus syndrome in the first 6 months of life. *British Journal of Ophthalmology* **86**: 670–675.

- Hoffmann MB, Seufert PS (2005) Simulated nystagmus reduces pattern-reversal more strongly than pattern-onset multifocal visual evoked potentials. *Clinical Neurophysiology* **116**: 1723–1732.
- Hoffmann MB, Seufert PS, Bach M (2004) Simulated nystagmus suppresses pattern-reversal but not pattern-onset visual evoked potentials. *Clinical Neurophysiology* **115**: 2659–2665.
- Kelly DH (1979) Motion and vision. II. Stabilized spatiotemporal threshold surface. *Journal of the Optical Society of America* **69**: 1340–1349.
- Leigh RJ, Zee DS (1991) *The Neurology of Eye Movements*, 2nd edn. Philadelphia, PA: FA Davis.
- Reinecke R, Guo S, Goldstein HP (1988) Waveform evolution in infantile nystagmus: an electrooculographic study of 35 cases. *Binocular Vision* **4**: 191–202.
- Saunders KJ, Brown G, McCulloch DL (1998) Pattern-onset visual evoked potentials: more useful than reversal for patients with nystagmus. *Documenta Ophthalmologica* **94**: 265–274.
- Shawkat FS, Kriss A, Russell-Eggitt I, Taylor D, Harris C (2001) Diagnosing children presenting with asymmetric pendular nystagmus. *Developmental Medicine & Child Neurology* **43**: 622–627.
- Westheimer G, McKee SP (1975) Visual acuity in the presence of retinal image motion. *Journal of the Optical Society of America* **65**: 847–850.